A rough-surface scattering function for Titan radar studies

Bruce A. Campbell[1]

[1]   Numerous studies show a relationship between radar backscattering and surface roughness. While estimating the statistical properties of small-scale topography is of particular interest for geologic analysis of Cassini radar data, there is no analytic description of radar scattering over a wide range of incidence angles and roughness. This paper presents an empirical function that links the rms slope at the horizontal scale of the wavelength and HH- or VV-polarization radar echoes. The model is based on comparison of 24-cm wavelength AIRSAR data for lava flows in Hawai'i, at incidence angles of 25° to 55°, with topographic profiles at 25-cm posting. Comparison of model predictions to the range of observed Titan echoes suggests that the radar return is often dominated by a component arising from subsurface scattering. **Citation:** Campbell, B. A. (2007), A rough-surface scattering function for Titan radar studies, *Geophys. Res. Lett.*, *34*, L14203, doi:10.1029/2007GL030442.

1.   Introduction

[2]   One major goal of radar remote sensing is to estimate the statistical properties of target surface topography. This is particularly important in studies of cloud-obscured terrain, such as on Venus and Titan. The link between the radar echo and roughness properties has long been a topic of study, but analytical representations of the scattering process remain limited to a suite of statistically well-defined surface models. In most planetary remote sensing studies, we do not know if the geology of a target region conforms to any such model. Useful geologic information may still be obtained by comparing radar observations to empirically derived functional relationships between echo strength and roughness parameters.

[3]   Radar backscatter from natural surfaces, at free-space wavelength λ, is modulated by topography at scales from about $\lambda/10$ and larger, the dielectric properties of the target region, the transmit and receive polarization states, and the observation geometry specified by the incidence angle, φ. Cassini SAR imaging of Titan ($\lambda = 2.17$ cm) uses an angular range of $20-35°$, and an arbitrary linear polarization that mixes the HH (horizontal-transmit, horizontal-receive) and VV (vertical-transmit, vertical-receive) states [*Elachi et al.*, 2004]. For comparison, Magellan measurements of Venus ($\lambda = 12.6$ cm) use incidence angles of $\sim22°-48°$, and either HH or VV polarization [*Saunders et al.*, 1992].

[4]   Theoretical treatments of radar scattering typically address either the near-nadir regime from normal incidence to $10-20°$ [e.g., *Hagfors*, 1964], where the reflection is dominated by locally smooth, radar-facing portions of the surface, or the region beyond $\varphi \sim 20°$ where diffuse scattering predominates. Diffuse echoes arise due to scattering by smaller facets and randomly oriented edges or other sharp topographic features [*Hagfors and Evans*, 1968; *Beckmann*, 1968; *Campbell et al.*, 1993]. Analytic solutions for surface backscatter are limited to cases where the roughness has particular statistical limits [e.g., *Barrick and Peake*, 1967; *Ulaby et al.*, 1982; *Fung et al.*, 1992]. The difficulty in applying such models to radar data for Venus or Titan is that, in many geologic settings, we are likely to encounter vertical structure of cm to tens of cm over similar horizontal scales. This type of wavelength-scale structure generates significant diffusely scattered radar echoes, which are not well represented by current theoretical models.

[5]   This paper presents an empirically derived relationship between like-polarized (HH or VV) radar echoes and surface roughness at the wavelength scale, based on comparison of airborne radar data and field-measured topography for lava flows in Hawaii. Section 2 describes the radar and topographic datasets. Sections 3 and 4 develop the model function, based on similar work for the cross-polarized component by *Campbell and Shepard* [1996], and discuss validity limits and applications to Cassini SAR data.

2.   AIRSAR Data and Field Topographic Measurements

[6]   The NASA/JPL airborne synthetic aperture radar (AIRSAR) system collects backscatter images with 5– 10 m resolution for wavelengths of 5.7, 24, and 68 cm. Every radar resolution cell is characterized by a Stokes scattering matrix, which can be used to generate echoes in any desired transmit/receive polarization state [*van Zyl et al.*, 1987]. The data used here cover the Kilauea Caldera and Ka'u Desert region in Hawai'i (Figure 1), which has minimal vegetation and a relatively narrow range of surface dielectric constant. Three approximately parallel flight lines were collected, so each field site is observed over a range of incidence angles from a low value of $25-30°$ to a high value of $50-55°$, depending upon location in the scene. The data were converted to values of the dimensionless backscatter coefficient, $\sigma°$, using field-deployed corner reflectors as calibration targets [*van Zyl*, 1990].

[7]   Topographic data for the ten field sites characterize cm-scale changes in elevation, $z(x)$, at 25-cm spacing over profile lengths of about 100 m [*Campbell and Shepard*, 1996]. The surface roughness varies from relatively slight on ponded pahoehoe flows to rugged, meter-scale plates and blocks that form a'a textures. A robust statistical description of topography data at some horizontal sampling interval, Δx, is the rms slope, $s(\Delta x)$ (Figure 2). The rms height, h, as

---

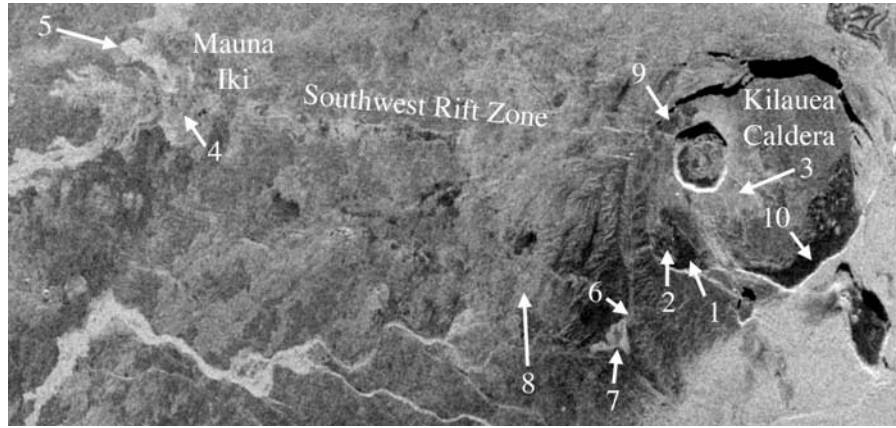[1]Center for Earth and Planetary Studies, Smithsonian Institution, Washington, D. C., USA.

Figure 1. VV-polarization, 24-cm wavelength AIRSAR image of Kilauea Caldera and the Ka'u Desert, Hawai'i. Radar incidence angle increases from top to bottom of image. Field sites for topography measurements are noted by number.

a function of profile length may also be calculated, but only at scales considerably larger than Δx [*Shepard et al.*, 2001]. The advantage of beginning an empirical analysis with the rms slope at the wavelength scale, rather than the rms height at some larger horizontal scale, is that we avoid the need for an explicit dependence on λ in the final model.

[8] The one-dimensional rms slope is defined as the ratio of the "Allen deviation", ν, to the horizontal sampling interval:

$$s(\Delta x) = \frac{\nu(\Delta x)}{\Delta x} = \frac{\sqrt{\left\langle [z(x) - z(x + \Delta x)]^2 \right\rangle}}{\Delta x} \quad (1)$$

and the "wavelength-scale rms slope" for a radar observation is $s(\lambda)$. Natural surfaces often follow a power-law relationship between the rms slope and the horizontal scale of measurement, characterized by the Hurst exponent, H:

$$s(\Delta x) = C_s \left(\frac{\Delta x}{\Delta x_o} \right)^{H-1} \quad (2)$$

where C_s is the rms slope at a reference length scale of Δx_o (typically 1 m). For the sites studied here, the measured Hurst exponents are between 0.26 and 0.68 (Table 1).

3. Empirical Radar Scattering Model

[9] One way to recover useful geologic information from radar data, without an analytic scattering model, is to construct functions based on airborne radar observations and field measurements of topography. This approach was successful in describing HV-polarized echoes with respect to the wavelength-scale rms slope [*Campbell and Shepard*, 1996]:

$$\sigma^o_{HV} = 0.04 \cos \phi \left[1 - e^{-1.7 s(\lambda)^2} \right] \quad (3)$$

Because the roughness parameter is scaled to λ, the same coefficients apply at all radar wavelengths.

[10] At the AIRSAR wavelengths, it is reasonable to assume that the HV-polarized echo arises predominantly

from surface scattering. This is supported by the good agreement between the model, derived from 24-cm data, and 68-cm echoes; if there were increasing HV subsurface echoes with increasing λ, we would see an overestimate of the surface roughness based on the 68-cm values [*Campbell and Shepard*, 1996]. This assumption is not necessarily valid for the HH and VV echoes, but can be checked by reference to the $\sigma^o_{HH}/\sigma^o_{VV}$ ratio. In general, radar scattering from moderately to very rough surfaces is characterized by $\sigma^o_{HH}/\sigma^o_{VV}$ values close to unity. $\sigma^o_{HH}/\sigma^o_{VV}$ values <1 are correlated with either a slightly rough surface, or with radar penetration and scattering by subsurface objects, voids, or interfaces [*Campbell et al.*, 2004]. There is no evidence for significant subsurface scattering at λ = 24 cm for the ten field sites ($\sigma^o_{HH}/\sigma^o_{VV} \sim 1$), but at 68-cm wavelength some of the smoother sites have values of $\sigma^o_{HH}/\sigma^o_{VV}$ < 1.

[11] The development of the empirical model begins by fitting a linear function between σ^o (in dB), and the incidence angle, φ (in degrees), for each field site (Table 1). This allows interpolation of σ^o_{HH} and σ^o_{VV} values for all ten sites at $\varphi = 20°–60°$. Since the HH- and VV-polarized
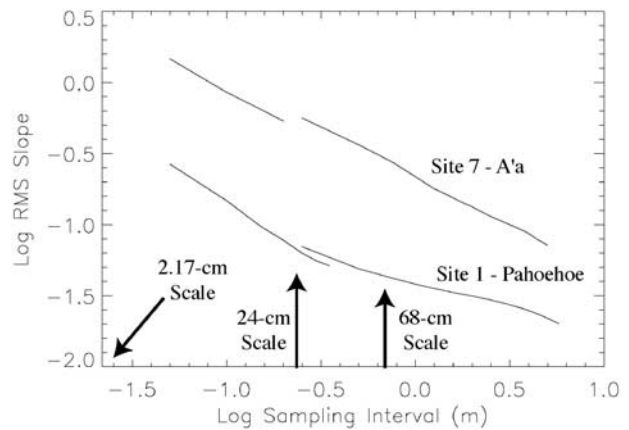

Figure 2. RMS slope of surface topography as a function of horizontal scale length for two lava flow study sites in Hawai'i. The curves for small-scale roughness on each flow come from 5-cm spacing profiles about 5 m long, and the larger-scale topography is constrained by 25-cm spacing profiles about 100 m long.

Table 1. Statistical and Radar Scattering Properties of Kilauea Field Sites[a]

Site	Description	H	s, 24 cm	s, 68 cm	C_h, m	σ° at 24-cm, dB
1	Ponded pahoehoe	0.62	0.073	0.044	0.014	$-12.52 - 0.247\varphi$
2	Ponded flows with tumuli	0.68	0.172	0.116	0.036	$-6.25 - 0.263\varphi$
3	Platy pahoehoe	0.51	0.436	0.263	0.085	$-1.95 - 0.210\varphi$
4	Billowy pahoehoe toes	0.48	0.324	0.193	0.062	$-3.65 - 0.193\varphi$
5	A'a	0.26	0.705	0.316	0.120	$-7.10 - 0.036\varphi$
6	Ropy pahoehoe	0.44	0.222	0.125	0.041	$-6.47 - 0.210\varphi$
7	A'a	0.29	0.586	0.295	0.105	$-9.37 - 0.050\varphi$
8	Pahoehoe sheet flows	0.49	0.225	0.135	0.046	$-1.45 - 0.222\varphi$
9	Pahoehoe sheet flows	0.64	0.147	0.104	0.032	$-8.53 - 0.205\varphi$
10	Ponded pahoehoe	0.63	0.076	0.055	0.017	$-16.28 - 0.185\varphi$

[a]Site numbers correspond to locations shown in Figure 1. Values of the Hurst exponent, H, for horizontal scales <2 m; rms slope, s, at 24- and 68-cm horizontal scales; and C_h, the rms height at 1-m profile length, derived using methods described by *Shepard et al.* [2001]. Backscatter function for average of HH- and VV-polarized echoes at 24-cm wavelength derived from linear fit between the backscatter coefficient (in dB) and incidence angle, φ (in degrees).

echoes are similar, they are averaged together to reduce noise. At each angle, a function of the form in (3), without the $\cos\varphi$ term, was fit to the σ° values (in linear form rather than dB). Initially, both coefficients were allowed to vary with φ, but the leading term solutions clustered within a narrow range about 0.16. The second coefficient exhibited an exponential dependence on incidence angle, with a best-fit behavior of $70.372e^{-0.0644\varphi}$. The complete function is thus (where σ° is in linear form, and φ is in degrees):

$$\sigma^o_{HH,VV} = 0.16\left[1 - \exp\left\{-70.372s(\lambda)^2 \exp(-0.0644\phi)\right\}\right] \quad (4)$$

[12] The model predicts well the backscattered echo at $\lambda = 24$ cm for the field sites (Figure 3), but the question remains as to whether this dependence on $s(\lambda)$ persists over a range of wavelength. While the rms slope at the wavelength scale is sufficient to predict HV-polarized echoes (3), the HH- and VV-polarized components could conceivably also depend upon the variation in roughness about this length scale described by the Hurst exponent. The 68-cm AIRSAR data provide a test of the model. Given the evidence of modest radar penetration at 68-cm wavelength, only the HH-polarized data are used, since they have a

smaller component of any subsurface echo [*Campbell et al.*, 2004]. The 68-cm σ°_{HH} values for the ten field sites predicted from the measured topography generally correlate with the observed σ° values, though with greater scatter for rougher surfaces than at 24-cm wavelength (Figure 3). Based on these data, it appears that the derived empirical function is not strongly dependent upon H, at least for surfaces with Hurst exponents around 0.5.

[13] Models for radar echoes from soil surfaces were derived by *Dubois et al.* [1995; J. van Zyl, corrections provided in a private communication, 2007] and *Oh et al.* [1992], using the rms height at 1-m horizontal scale (here termed C_h) as the roughness parameter. The variation of backscatter with wavelength given by *Dubois et al.* [1995] has a fixed power-law form, which may be interpreted as a means to extrapolate C_h to the range of horizontal scales (i.e., radar wavelengths) used in the study. Both models have a uniform dependence of σ° on incidence angle, where the model proposed here allows the angular scattering function to have a shallower slope with φ for rougher terrain (Figure 4). The *Oh et al.* [1992] model is in good agreement with the Hawaii 24-cm data (Table 1) for smoother areas, but underestimates σ° for rough terrain. The *Dubois et al.*
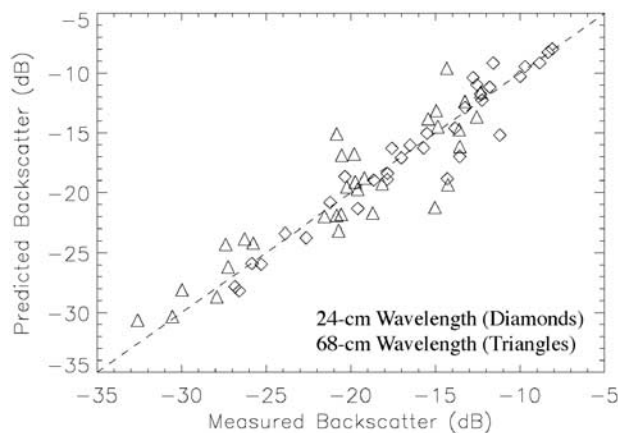
Figure 3. Comparison of empirical scattering function predictions to observed radar backscatter coefficient for 24-cm and 68-cm wavelength data. Comparisons made for backscatter coefficients at three incidence angle values for each of the ten field sites.
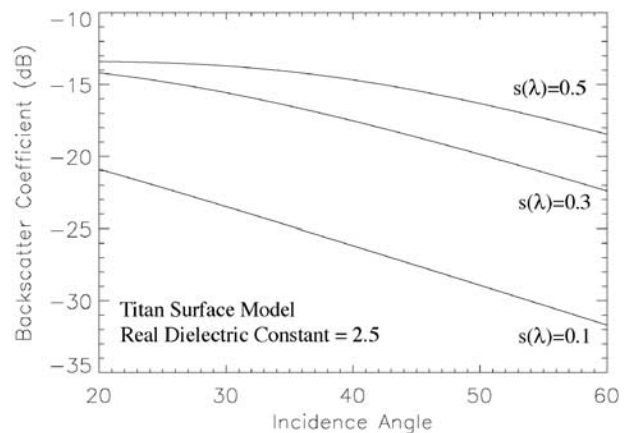
Figure 4. Predicted radar backscatter coefficient versus incidence angle for Titan surface, with a real dielectric constant of 2.5, at three values of the wavelength-scale rms slope. The maximum value of -13.4 dB corresponds to a completely diffuse-scattering surface.

[1995] model overestimates the backscatter by 1–3 dB for rough surfaces and by 5–7 dB for smooth surfaces.

[14]　In order to use the model in (4) for planetary remote sensing, we must account for any difference between the reflectivity of the target surfaces and the Kilauea flows. The backscattered return from natural surfaces often is assumed linearly related to the Fresnel normal reflectivity, ρ_o [e.g., *Hagfors*, 1964; *Barrick and Peake*, 1967], suggesting that the leading coefficient in (4) implicitly includes this term. The asymptotic value of the scattering function is inferred to correspond to a surface that distributes the reflected power in any given polarization state uniformly into the hemisphere above the target. The backscatter coefficient is normalized to the behavior of a conducting interface that scatters incident energy uniformly above the surface, so a dielectric target that preserves the sense of incident polarization has $\sigma^\circ = \rho_o$. This value is reduced by the degree to which the incident energy is changed in polarization (i.e., HV echoes rather than HH). A collection of randomly oriented, dipole-like scattering elements depolarizes 25% of the incident energy, so the leading coefficient in (4) is $0.75\rho_o$, corresponding to a real dielectric constant of about 7. This is at the high end of the measured range for Kilauea basalts, and contrasts with a value of 5.4 obtained from analysis of the HV-polarized echoes [*Campbell and Shepard*, 1996]. Taking a value of $\varepsilon' = 6$ ($\rho_o = 0.177$) as a good approximation, the HH- or VV-polarization scattering function (4) may be written as:

$$\sigma^o_{HH,VV} = 0.9\rho_0\left[1 - \exp\left\{-70.372 s(\lambda)^2 \exp(-0.0644\phi)\right\}\right] \quad (5)$$

and the wavelength-scale rms slope is given by:

$$s(\lambda) = \left[\frac{e^{0.0644\phi}}{-70.372}\ln\left[1 - \frac{\sigma^o}{0.9\rho_o}\right]\right]^{1/2} \quad (6)$$

While the behavior of the radar echo as a function of incidence angle and roughness is well represented by the expression inside the brackets in (5), the leading coefficient has an uncertainty related to the estimated reflectivity of the field sites and to any calibration errors in the AIRSAR data. Extremely smooth surfaces have differences in HH- and VV-polarized echoes that are not reflected in this approximation [e.g., *Oh et al.*, 1992; *Campbell et al.*, 2004].

4. Application to Titan Remote Sensing

[15]　Most surfaces on Titan appear to have real dielectric constants ranging from 2–3, consistent with the expected water-ammonia ices and hydrocarbon materials [*Elachi et al.*, 2005; *Wye et al.*, 2007]. Taking the middle of this range, ρ_o is 0.05, yielding the radar backscatter values as a function of φ and $s(\lambda)$ shown in Figure 4. The Cassini radar "noise floor" is $\sigma^\circ = -25$ dB [*Elachi et al.*, 2004]. For $\varepsilon' = 2.5$, this corresponds to a wavelength-scale rms slope (6) of 0.06 (3.4°) at $\varphi = 20°$, and 0.12 (7°) at $\varphi = 40°$. These are low values relative to even very smooth terrestrial surfaces (Figure 2), supporting the notion that areas on Titan with echoes near the noise floor are bodies of standing liquid [*Stofan et al.*, 2007].

[16]　At the higher end of possible roughness, the asymptotic value of the estimated Titan surface scattering function is $\sigma^\circ = -13.4$ dB. Many areas have backscatter coefficients well above this value [e.g., *Stofan et al.*, 2006, 2007], suggesting two possible scenarios. Multiple scattering interactions among portions of the surface that are locally smooth at the wavelength scale can produce an enhancement in the backscatter strength, as observed for blocky terrestrial lava flows [*Campbell et al.*, 1993; *Plaut et al.*, 2004]. This seems unlikely given the large areas over which the high backscatter occurs. A more reasonable explanation is that much of the variability in radar brightness observed in Titan SAR data is due to changes in volume scattering beneath a surface that is entirely diffuse in its scattering behavior.

[17]　The possibility of a volume scattering component in the Titan radar echoes has been suggested in other analyses, based in part on radiometric properties measured by the radar receiver [*Elachi et al.*, 2005; *Wye et al.*, 2007; *Paillou et al.*, 2006]. That volume scattering in a low-loss medium can lead to strong backscattered returns is supported by observations of the icy moons of Jupiter [*Ostro et al.*, 1992; *Black et al.*, 2001], and by analysis of AIRSAR data for the Greenland ice sheet [*Rignot*, 1995]. The model presented here sets an upper limit on the topography-related component of the HH- or VV-polarized echo, and thus offers a means to estimate the relative roles of surface and volume scattering.

References

Barrick, D. E., and W. H. Peake (1967), Scattering from surfaces with different roughness scales: Analysis and interpretation, *Ohio State Univ. Electrosci. Lab. Rep. 1388-26*, Ohio State Univ., Columbus.

Beckmann, P. (1968), *Depolarization of Electromagnetic Waves*, Golem Press, Boulder, Colo.

Black, G. J., D. B. Campbell, and P. D. Nicholson (2001), Icy Galilean satellites: Modeling radar reflectivities as a coherent backscatter effect, *Icarus*, *151*, 167–180.

Campbell, B. A., and M. K. Shepard (1996), Lava flow surface roughness and depolarized radar scattering, *J. Geophys. Res.*, *101*, 18,941–18,952.

Campbell, B. A., R. E. Arvidson, and M. K. Shepard (1993), Radar polarization properties of volcanic and playa surfaces: Applications to terrestrial remote sensing and Magellan data interpretation, *J. Geophys. Res.*, *98*, 17,099–17,114.

Campbell, B. A., T. A. Maxwell, and A. Freeman (2004), Mars orbital synthetic aperture radar: Obtaining geologic information from radar polarimetry, *J. Geophys. Res.*, *109*, E07008, doi:10.1029/2004JE002264.

Dubois, P. C., J. J. van Zyl, and T. Engman (1995), Measuring soil moisture with imaging radars, *IEEE Trans. Geosci. Remote Sens.*, *33*, 915–926.

Elachi, C., et al. (2004), RADAR: The Cassini Titan RADAR Mapper, *Space Sci. Rev.*, *115*, 71–110.

Elachi, C., et al. (2005), Cassini radar views the surface of Titan, *Science*, *308*, 970–974.

Fung, A. K., Z. Li, and K. S. Chen (1992), Backscattering from a randomly rough dielectric surface, *IEEE Trans. Geosci. Remote Sens.*, *30*, 356–369.

Hagfors, T. (1964), Backscattering from an undulating surface with applications to radar returns from the Moon, *J. Geophys. Res.*, *69*, 3779–3784.

Hagfors, T., and J. V. Evans (1968), Radar studies of the Moon, in *Radar Astronomy*, edited by T. Hagfors and J. V. Evans, pp. 219–273, McGraw-Hill, New York.

Oh, Y., K. Sarabandi, and F. T. Ulaby (1992), An empirical model and an inversion technique for radar scattering from bare soil surfaces, *IEEE Trans. Geosci. Remote Sens.*, *30*, 370–381.

Ostro, S. J., et al. (1992), Europa, Ganymede, and Callisto: New radar results from Arecibo and Goldstone, *J. Geophys. Res.*, *97*, 18,227–18,244.

Paillou, P., M. Crapeau, C. Elachi, S. Wall, and P. Encrenaz (2006), Models of synthetic aperture radar backscattering for bright flows and dark spots on Titan, *J. Geophys. Res.*, *111*, E11011, doi:10.1029/2006JE002724.

Plaut, J. J., S. W. Anderson, D. A. Crown, E. R. Stofan, and J. van Zyl (2004), The unique radar properties of silicic lava domes, *J. Geophys. Res.*, *109*, E03001, doi:10.1029/2002JE002017.

Rignot, E. (1995), Backscatter model for the unusual radar properties of the Greenland Ice Sheet, *J. Geophys. Res.*, *100*, 9389–9400.

Saunders, R. S., et al. (1992), Magellan mission summary, *J. Geophys. Res.*, *97*, 13,067–13,090.

Shepard, M. K., B. A. Campbell, M. Bulmer, T. Farr, L. R. Gaddis, and J. Plaut (2001), The roughness of natural terrain: A planetary and remote sensing perspective, *J. Geophys. Res.*, *106*, 32,777–32,795.

Stofan, E. R., et al. (2006), Mapping of Titan: Results from the first Titan radar passes, *Icarus*, *185*, 443–456.

Stofan, E. R., et al. (2007), The lakes of Titan, *Nature*, *445*, 61–64.

Ulaby, F. T., R. K. Moore, and A. K. Fung (1982), *Microwave Remote Sensing*, Addison-Wesley, Reading, Mass.

van Zyl, J. J. (1990), Calibration of polarimetric radar images using only image parameters and trihedral corner reflectors, *IEEE Trans. Geosci. Remote Sens.*, *28*, 337–348.

van Zyl, J. J., H. A. Zebker, and C. Elachi (1987), Imaging radar polarization signatures: Theory and observations, *Radio Sci.*, *22*, 529–543.

Wye, L. C., et al. (2007), Electrical properties of Titan's surface from Cassini RADAR scatterometer measurements, *Icarus*, *188*, 367–385, doi:10.1016/j.icarus.2006.12.008.

_____

B. A. Campbell, Center for Earth and Planetary Studies, Smithsonian Institution, MRC 315, P.O. Box 37012, Washington, DC 20013-7012, USA. (campbellb@si.edu)